Molybdenum and tungsten in sapphire crystal growth industry

M. Mark*, H. Traxler*, R. Schiftner*, B. Kleinpaß*, W. Knabl*

* Plansee SE, 6600 Reutte, Austria

Abstract

High-temperature refractory metals such as molybdenum- and tungsten-based materials are essential in today's sapphire crystal growing technologies and are widely used for crucibles, hot-zone shieldings or heaters. The worldwide sapphire production capacities are dominated by the three growing methods Kyropoulos process, heat-exchange method and edged-defined film-fed growth. The key for economic success of all these methods lies in high-quality, large-size crystals while keeping production costs as low as possible. Consequently, performance and lifetime of high-melting metal components are crucial for cost reduction in this competitive market.

The paper gives a broad insight into high-temperature characteristics of molybdenum, tungsten and their alloys. The discussion focuses on mechanical and thermo-physical properties, and on interactions of liquid alumina with refractory metals at 2100 °C. We propose MoW as an interesting alloy with high creep resistance and modified thermo-physical behavior. Additional efforts on conditioning refractory metal surfaces in contact with melts could boost particularly crucible lifetimes.

Keywords

Sapphire, Crystal Growth, Molybdenum, Tungsten, Tensile Test, Yield Strength, Melt Resistance, Gas Bubbles, Wetting Angle

Introduction

Sapphire is a hard, wear resistant and strong material with a high melting temperature, it is chemically widely inert, and it shows interesting optical properties. Therefore, sapphire is used for many technological applications where the main industry fields are optics and electronics. Today the largest fraction of industrial sapphire is used as a substrate for the LED and semiconductor production, followed by usage as windows for watches, mobile phone parts or bar code scanners, to name a few examples [1]. Today, various methods to grow sapphire single crystals are available, a good overview can be found e.g. in [1, 2]. However, the three growing methods Kyropoulos process (KY), heat-exchange method (HEM) and edged-defined film-fed growth (EFG) account for more than 90 % of the worldwide sapphire production capacities.

The first attempt for a synthetically produced crystal has been made 1877 for small ruby single crystals [2]. Readily in 1926 the Kyropoulos process was invented. It operates in vacuum and allows to produce large cylindrical shape boules of very high quality. Another interesting sapphire growing method is the edge-defined film-fed growth. The EFG technique is based on a capillary channel which is filled with liquid-melt and allows to grow shaped sapphire crystals such as rods, tubes or sheets (also called ribbons). In contrast to these methods the heat-exchange method, born in the late 1960's, allows to grow large sapphire boules inside a spun crucible in the shape of the crucible by defined heat extraction from the bottom. Because the sapphire boule sticks to the crucible at the end of the growing process, boules can crack at the cool down process and the crucible can only be used once.

Any of these sapphire crystal growing technologies have in common that core components – particularly crucibles – are requiring high-temperature refractory metals. Depending on the growing method crucibles are made of molybdenum or tungsten, but the metals are also widely used for resistance heaters, die-packs and hot-zone shieldings [1]. However, in this paper we focus our discussion on KY and EFG related topics since pressed-sintered crucibles are used in these processes.

In this report we present material characterization studies and investigations on surface conditioning of pressed-sintered materials such as molybdenum (Mo), tungsten (W) and its alloys (MoW). In the first part our focus lies on high-temperature mechanical data and ductile to brittle transition temperature. Complementary to mechanical properties we have studied thermo-physical properties, i.e. the coefficient of thermal expansion and thermal conductivity. In the second part we present studies on a surface conditioning technique specifically to improve the resistance of crucibles filled with alumina melt. In the third part we report on measurements of wetting angles of liquid alumina on refractory metals at 2100 °C. We carried out melt-drop experiments on Mo, W and MoW25 alloy (75 wt.% molybdenum, 25 wt.% tungsten) and studied dependencies on different atmospheric conditions. As a result from our investigations we propose MoW as an interesting material in sapphire growth technologies and as a potential alternative to pure molybdenum and tungsten.

High-temperature mechanical and thermo-physical properties

The sapphire crystal growth methods KY and EFG readily serve for more than 85 % of the worlds sapphire quantity share. In both methods, the liquid alumina is placed in pressed-sintered crucibles, typically made of tungsten for the KY process and made of molybdenum for the EFG process. Crucibles are critical system parts for these growing processes. Aiming the idea to possibly reduce the costs of tungsten crucibles in the KY process as well as increase the lifetime of molybdenum crucibles in the EFG process, we produced and tested additionally two MoW alloys, i.e. MoW30 containing 70 wt.% Mo and 30 wt.% W and MoW50 containing 50 wt.% Mo and W each.

For all material characterization studies we produced pressed-sintered ingots of Mo, MoW30, MoW50 and W. Table I shows densities and average grain sizes corresponding to the initial material states.

Table I: Summary of pressed-sintered materials used for the measurements on mechanical and thermo-physical properties. The table shows the density and average grain size of the initial states of the materials.

Material	density (g/cm³)	Relative density (%)	Average grain size (µm)
Mo	9.7	95.1	23
MoW30	11.6	97.2	18
MoW50	12.8	96.0	16
W	18.1	93.9	21

Because crucibles are long-time exposed to high temperatures, we conducted elaborate tensile tests particularly in the high-temperatures range between 1000 °C and 2100 °C. Figure 1 summarizes these results for Mo, MoW30, and MoW50 where the 0.2 % yield strength ($R_{p0.2}$) and the elongation to fracture (A) is shown. For comparison, a data point of pressed-sintered W is indicated at 2100 °C.

For ideal solid-soluted tungsten in molybdenum the $R_{p0.2}$ is expected to increase compared to pure Mo material. For temperatures up to 1800 °C both MoW alloys show at least 2 times higher $R_{p0.2}$ than for Mo, see Figure 1(a). For higher temperatures only MoW50 shows a significantly improved $R_{p0.2}$. Pressed-sintered W shows the highest $R_{p0.2}$ at 2100 °C. The tensile tests reveal also A as shown in Figure 1(b). Both MoW alloys show very similar elongation to fracture values which are typically half the values of Mo. The relatively high A of tungsten at 2100 °C should be caused by its more fine-grained structure as compared to Mo.

To determine the ductile to brittle transition temperature (DBTT) of the pressed-sintered molybdenum tungsten alloys, also measurements on the bending angle were conducted at various testing temperatures. The results are shown in Figure 2. The DBTT increases with increasing tungsten content. While the DBTT of Mo is relatively low at about 250 °C, the alloys MoW30 and MoW50 show a DBTT of approximately 450 °C and 550 °C, respectively.

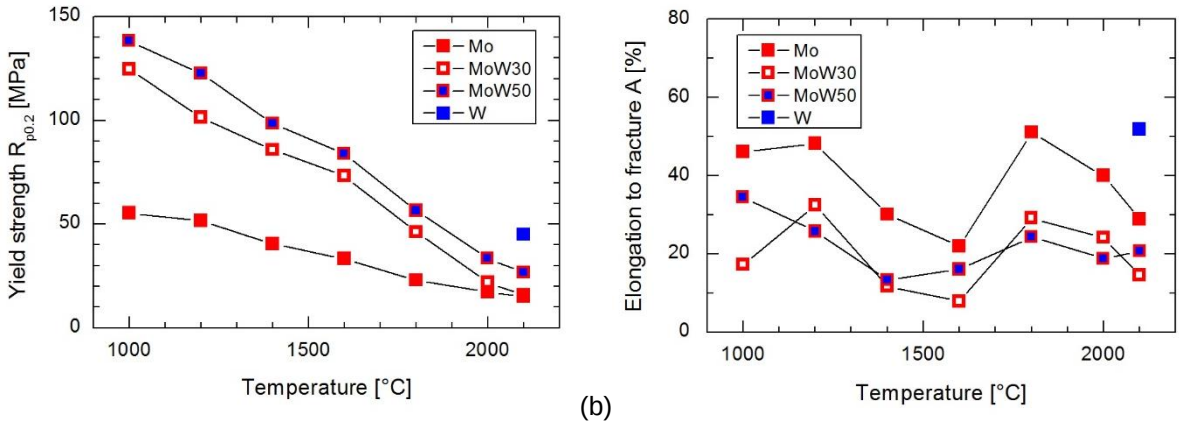

Figure 1: Measurement results of tensile tests of various pressed-sintered molybdenum tungsten alloys as a function of testing temperature with (a) showing the yield strength and (b) the elongation to fracture. All data are average values of 3 individual measurements, the statistical error is within the size of the data points.

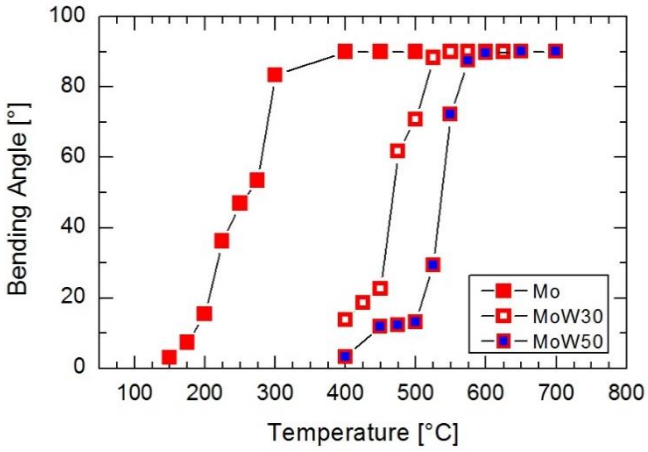

Figure 2: Measurements of the bending angle for various pressed-sintered molybdenum tungsten alloys as a function of the testing temperature to determine the ductile to brittle transition of the materials. All data are average values of at least 3 individual measurements. The statistical error of the bending angle is largest in the transition range and maximum 20 %.

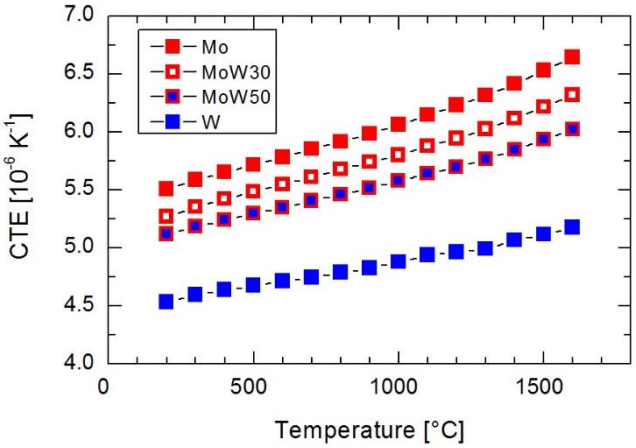

Figure 3: Coefficient of thermal expansion of various pressed-sintered molybdenum tungsten alloys as a function of testing temperature. The data are average values of 3 measurements on separate specimen. The statistical error is about 2 %.

Complementary to the mechanical characterization we also studied thermo-physical properties. The coefficient of thermal expansion (CTE) was measured in a push-rod dilatometer [3] in a temperature range up to 1600 °C using specimen with Ø5 mm and 25 mm length. The CTE measurements are illustrated in Figure 3. All materials show a very similar dependency of the CTE with increasing temperature. The CTE values for the alloys MoW30 and MoW50 are between the values of Mo and W. Because the residual porosity of the pressed-sintered materials is discontiguous and with small individual pores, the obtained CTE is similar to high-density materials such as sheets and rods [4].

The thermal conductivity of the pressed-sintered materials was obtained by measuring both the thermal diffusivity and the specific heat of specimen with Ø12.7 mm and 3.5 mm thickness using the laser flash method [5, 6]. For isotropic materials, such as pressed-sintered materials, the specific heat can be measured with the same method. The measurements have been taken in the temperature range between 25 °C and 1000 °C. To calculate the thermal conductivity we used in addition the material densities as shown in Table I and assume temperature independent densities. Figure 4 shows the resulting thermal conductivity for pressed-sintered Mo, MoW30, MoW50 and W. The thermal conductivity

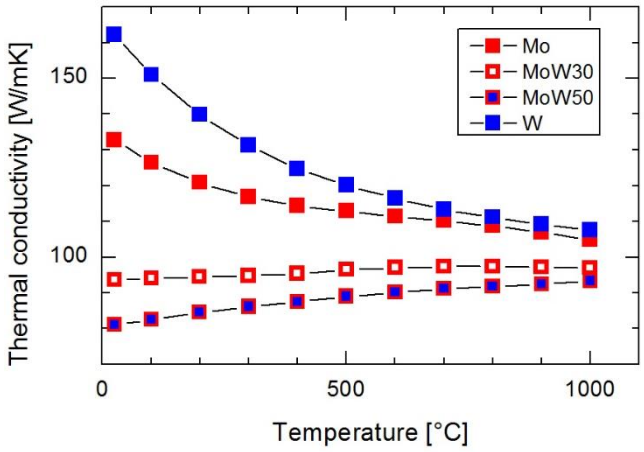

Figure 4: Thermal conductivity of various pressed-sintered molybdenum tungsten alloys as a function of the testing temperature. The data are based on calculations using average values of thermal diffusivity and specific heat as well as the materials' densities at room temperature from 3 measurements. The resulting overall uncertainty is 10 %.

of MoW alloys is lower than 100 W/mK for all temperatures investigated and much smaller as compared to pure molybdenum and tungsten. In addition, the conductivities of Mo and W decrease with increasing temperature while the conductivity of the MoW alloy indicates increasing values with increasing temperature.

The reason for this difference has not been investigated in this work and will be part of future investigations. It is known that for metals the dominating part of the thermal conductivity at low temperatures is the phonon contribution while at high temperatures the electron gas dominates the thermal conductivity [7]. Phonons are affected by material imperfections and defects. However, the increase of the thermal conductivity in the low temperature range is observed not only for MoW alloys but also for other solid-solution materials such as e.g. tungsten-rhenium [8], where the electron contribution plays an important role.

The comparison of the mechanical and thermo-physical properties shows that MoW is an interesting material for sapphire applications. For high temperatures > 2000 °C the yield strength is higher than for molybdenum and longer lifetimes of crucibles should be feasible. However, the material becomes more brittle and machining and handling should be adjusted. The significantly reduced thermal conductivity of pressed-sintered MoW as shown in Figure 4 indicates that adapted heat-up and cool-down parameters of the growing furnace might be necessary. Particularly in the heat-up phase, where alumina needs to be melted in the crucible, heat is transported only by the crucible to its raw filling material. The reduced thermal conductivity of MoW should be considered to avoid high thermal stress in the crucible. The range of the CTE values of MoW alloys is interesting in context of the HEM crystal growing method. As discussed in reference [9] the CTE of Mo is causing the clamping of the sapphire in the cool down phase. Therefore, the reduced CTE of MoW alloy might be the key to realize re-useable spun crucibles for the HEM process.

Surface conditioning of pressed-sintered refractory metals

As discussed in the introduction, pressed-sintered crucibles are often used in sapphire crystal growth processes to heat and keep the alumina melt slightly above 2050 °C. One important requirement for final

sapphire crystal quality is to keep impurities and gas bubbles in the melt as low as possible. Pressed-sintered parts do have a residual porosity and show a fine-grained structure. This fine-grained structure with closed porosity is fragile to enhanced corrosion of the metal particularly by oxidic melts. Another problem for sapphire crystals are small gas bubbles within the melt. The formation of gas bubbles is enhanced by increased surface roughness of the refractory part which is in contact with the melt.

To overcome these issues of pressed-sintered materials we exploit a mechanical surface treatment. We tested the method with a pressing tool where a ceramic device is working the surface under a defined pressure of a pressed-sintered part [10]. The effective pressing stress on the surface is inversely depending on the contact surface of the ceramic tool during this surface conditioning. With this treatment a high pressing stress can be locally applied to the surface of pressed-sintered materials and the material surface is plastically deformed. Figure 5 shows an example of a pressed-sintered molybdenum specimen which has been worked with this technique.

Figure 6 shows qualitatively the dependence of the effective pressing stress on the tool pressure. The data were derived from measurements of static imprints of the tool in pressed-sintered molybdenum. The line represents the fit to the data according to our model.

Figure 5: Mirror-like surface of a surface conditioned pressed-sintered Mo sample.

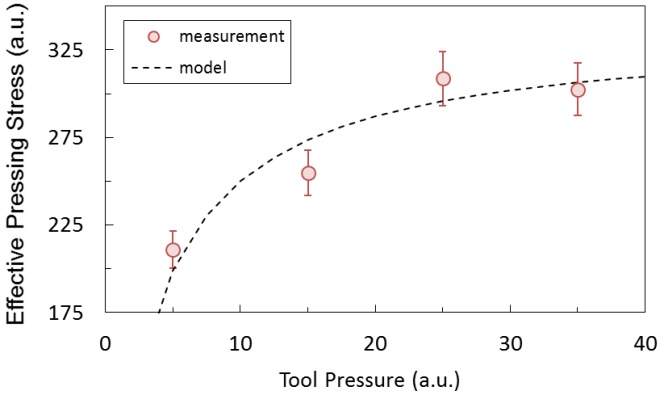

Figure 6: Effective pressing stress as a function of the tool pressure on pressed-sintered molybdenum. The error bars are estimated with 5 %.

Figure 7 shows the analysis results summarized for the surface roughness and surface hardness measurements as a function of the tool pressure for various pressed-sintered materials prepared as disks. As shown in Figure 7(a) the treatment results in a hardening of the surface. The hardness of both tested materials Mo and MoW30 is increased by about 150 %. For high tool pressures the hardness is not further increasing. Figure 7(b) shows that highly smooth surfaces with R_a as low as 0.1 µm for Mo are possible. For increasing tool pressures the roughness of Mo increases again. Because the MoW30 (and W) are harder materials than Mo, the attained R_a values of MoW30 and W are generally 2-3 times higher than of Mo. In contradiction to Mo, the surface roughness of W decreases by applying higher tool pressures within the tested parameter range.

Our scanning electron microscopy (SEM) studies of the conditioned surfaces confirm the data of the surface roughness, see Figure 7(b). As depicted in Figure 8(a), particularly high tool pressures can lead to grain surface damages and microcracks. Conditioning at very high surface stress can cause even grain removal from the surface, see Figure 8(b). Similar effects can also be observed for MoW and W at certain machining parameters.

To study the effect of the surface conditioning technique with regard to the surface grain structure and its temperature behavior, we prepared annealing samples from the three test disks of Mo, MoW30 and W.

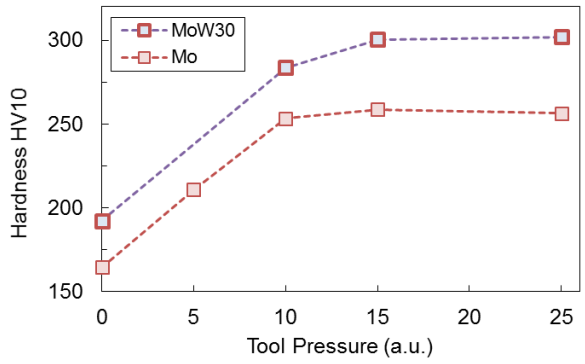

(a)

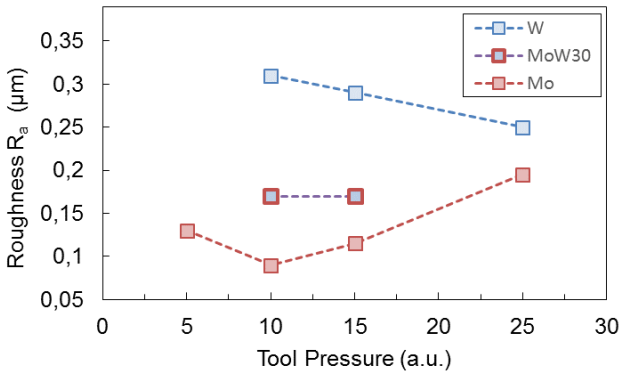

(b)

Figure 7: Surface roughness and hardness as a function of the applied tool pressure of pressed-sintered materials. (a) The hardness HV10 of the conditioned surface. (b) The surface roughness measured in radial direction on a length of 5.6 mm. The initial surface roughness of any material is about 0.8 µm. All data are averages of 3 measurements.

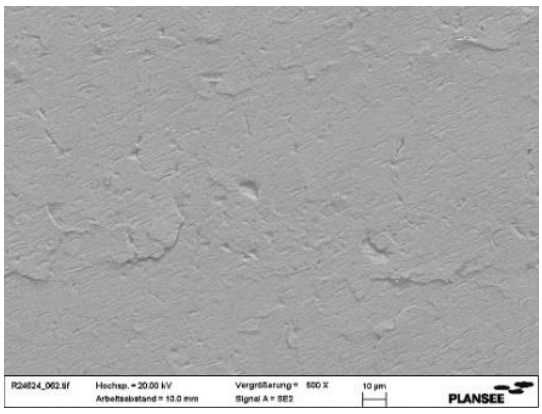

(a)

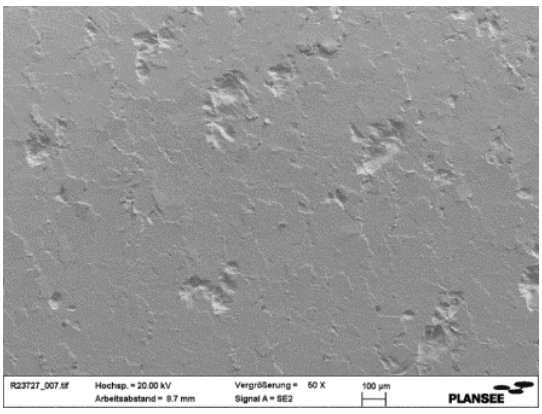

(b)

Figure 8: Examples of SEM images of Mo with conditioned surfaces at high tool pressures with (a) microcracks and (b) grain removal.

The samples were treated for 2 hours at different testing temperatures in the range 800 °C to 2000 °C and microsections were prepared for light microscopy analysis.

Figure 9 shows microsection examples of pressed-sintered molybdenum. The initial state of the treated surface is presented in Figure 9(a). The surface shows an almost dense layer within a range of about 200 µm. Below this layer a typical material structure with sintering pores is visible, the residual porosity is about 5 %. The measured residual porosity within the surface layer is well below 1 %. Figure 9(b) shows the grain structure after annealing for 2 h at 1700 °C. The thickness of the dense surface layer has increased and the grains are substantially larger than the grains in the volume not modified by surface conditioning. This coarse-grained highly dense layer will be effective to improve the creep resistance of the material.

We have studied the temperature dependence of the surface layer with regard to the thickness and the grain size for various tool pressures. Figure 10 shows representative examples for the surface layer thickness for Mo and MoW30. As illustrated in Figure 10(a) the initial surface layer thickness depends on the machining tool setup. At an annealing temperature above 800 °C the surface layer thickness of Mo starts to increase. At 2000 °C the layer thickness reaches values of 0.3 to 0.7 mm. For MoW30 an increase of the surface layer thickness can only be observed for temperatures above 1500 °C as shown Figure 10(b). Nevertheless at 2000 °C the layer thickness of MoW30 is very similar to Mo.

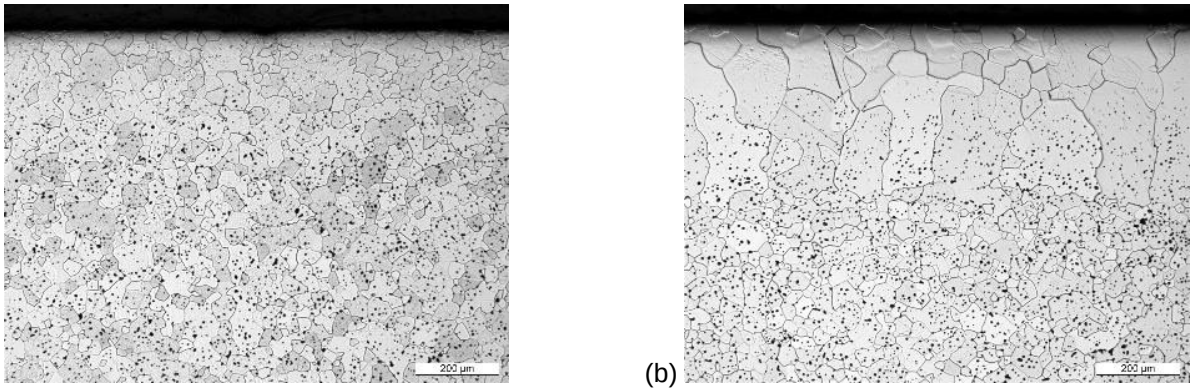

Figure 9: Example of microsections of pressed-sintered Mo with conditioned surface with (a) the initial state after treatment and (b) after 2 h annealing at 1700 °C.

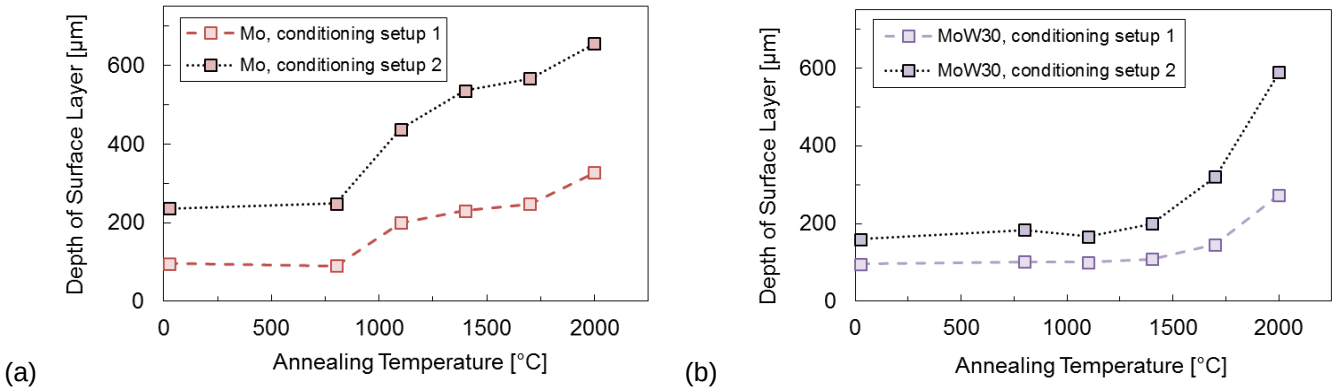

Figure 10: Thickness of surface layer as a function of annealing temperatures (a) for Mo and (b) for MoW30 obtained from microsection images.

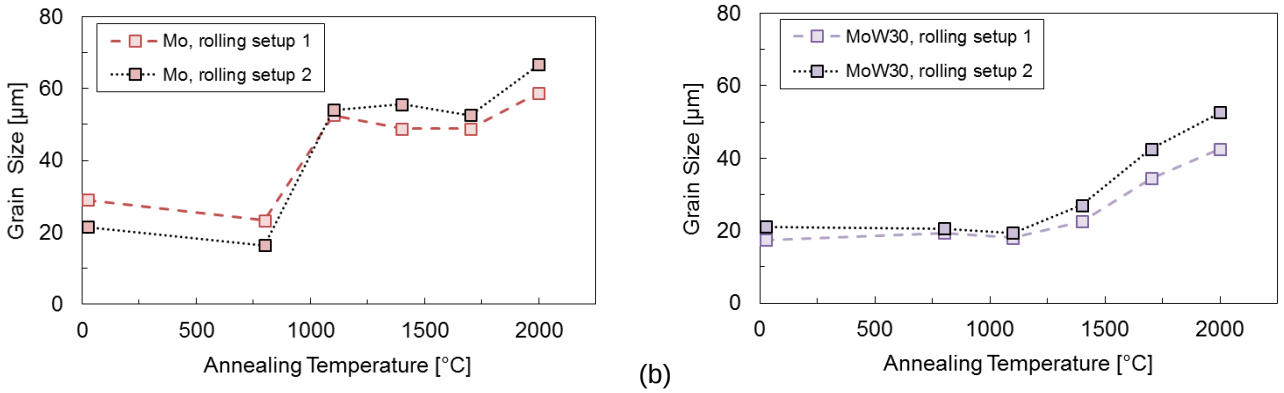

Figure 11: Average grain size of the surface layer as a function of annealing temperatures (a) for Mo and (b) for MoW30 obtained from microsection images.

Like the thickness analysis of the surface layer, Figure 11 shows average grain size data for Mo and MoW30 measured in the surface layer as a function of annealing temperatures. As can be inferred from the figures, the grain size is - within the measurement uncertainty - independent of the applied parameter setup. The grain size growth indicates an abnormal grain growth of the surface layer caused by the deformation of the surface area. Molybdenum grains grow at test temperatures above 1100 °C and the grain size is almost 3 times larger at 2000 °C compared to the initial grain size. MoW30 grains of the surface conditioned layer start to grow above temperatures of 1500 °C. At a test temperature of 2000 °C the average grain size is about 2 times the initial grain size.

In summary, our investigations on the surface conditioning technique show it is well applicable for pressed-sintered molybdenum tungsten alloys. Using this method, surfaces with increased hardness as well as smooth surfaces with R_a well below 0.5 µm can be obtained. The latter property is particularly beneficial for gas bubble reduction. The residual porosity in the surface layer is close to zero. Annealing and microsection studies show that a highly dense surface layer with a typical thickness of 500 µm can be obtained. Hereby the machining parameter can control the layer thickness. When exposing the conditioned material to high temperatures as typically used in sapphire growing methods, the surface layer becomes coarse-grained with grain size 2–3 times larger than without surface machining. The grain size in the surface layer is independent of machining parameters. The number of grain boundaries on the surface is effectively reduced. This leads to a higher resistance against diffusion of elements along grain boundaries and the melt attack is lower. Additionally, the high temperature creep resistance of pressed-sintered molybdenum tungsten alloys is improved.

Wetting studies of liquid alumina on refractory metals

The wetting of liquid alumina on molybdenum or tungsten is of fundamental interest in sapphire industry. Particularly for the EFG process the alumina wetting behavior in die-pack capillaries determine the growth rate of sapphire rods or ribbons. To understand the impact of selected material, surface roughness or process atmosphere we conducted detailed wetting angle measurements [11].

For the wetting measurements test substrates with a size of 1 x 5 x 40 mm³ were produced from Mo, MoW25 and W sheet materials. By sending high electric current through the metal sheet substrate the melting temperature of alumina of 2050 °C can be achieved within half a minute. For the angle measurements small alumina particles were placed on top of the sheet samples and subsequently

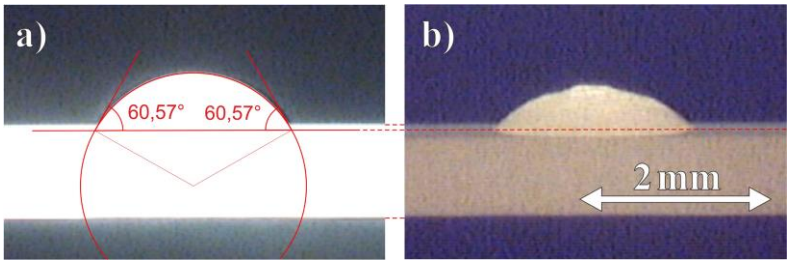

Figure 12: Example of the graphical measurement for wetting angles of tungsten by using (a) the image with the liquid melt droplet and (b) an image where the contour of the substrate (serving as a baseline) can be seen.

melted into droplets. An automated imaging system recorded the melt droplet as illustrated for example in Figure 12. Each melt-drop experiment allows to measure the wetting angle by analyzing the droplet contour, see Figure 12(a), and the substrate baseline usually shortly after turning off the heating current, see Figure 12(b).

We conducted wetting angle measurements for two different atmosphere conditions, vacuum at 10^{-5}mbar and argon at 900 mbar pressure. In addition, two surface types were tested, i.e. rough surfaces with R_a ~ 1 µm and smooth surfaces with R_a ~ 0.1 µm.

Table II summarizes the results of all measurements on the wetting angles for Mo, MoW25 and W for smooth surfaces. In general, the wetting angle of Mo is smallest as compared to the other materials. This implies that alumina melt is wetting Mo best which is beneficial in the EFG growing technique. The wetting angles obtained for argon are significantly lower than the angles for vacuum. For rough substrate surfaces we find systematically somewhat lower wetting angles. These values are typically about 2° lower than the angles given in Table II. However, because of the measurement uncertainty, no significant angle difference between smooth and rough surfaces can be reported.

Table II: Result of wetting angle measurements for smooth surfaces of three materials and for two atmospheres, vacuum (10-5 mbar) and argon (900 mbar). The data are averages of 6 angle values obtained from 3 measurements on separate droplets. The typical standard deviation of the measurements is 1-2 degree.

Material	Wetting angle in vacuum (deg.)	Wetting angle in argon (deg.)
Mo	52	42
MoW25	54	45
W	59	51

We measured wetting angles also for other atmosphere pressures, i.e. values between 10^{-5} mbar and 900 mbar. The preliminary analysis shows that for pressures between 10^{-5} mbar and 1 mbar the wetting angel does not change. Only above 1 mbar the wetting angle becomes lower than observed at 900 mbar argon (Table II). Beside the atmospheric condition, another important factor for the wetting behavior of alumina melt is the oxygen partial pressure. Our tests suggest that chemical interactions between the melt and the metal substrates occur within the complete measurement duration (typically 1 minute). We suspect dissolving processes of the Al_2O_3 molecules into other oxygen components which interact with

the substrate material near the melt droplet. Further studies are currently ongoing to investigate in more detail both the pressure dependence of the wetting angle and the chemical interactions of the melt with refractory metals.

Summary

Today's modern sapphire production technologies require the production of high-quality, large-size crystals at optimized production costs. The continuous improvement of high-temperature components for sapphire crystal growth is the key to increase the lifetime of refractory components and to produce single crystals with a minimum of impurities and defects. Our studies on the mechanical and thermo-physical properties of pressed-sintered materials show that MoW alloys are an interesting alternative material to be used in sapphire applications. The addition of W to Mo increases the high-temperature strength significantly. Therefore, deformation issues of Mo crucibles observed during the long running crystal growth cycle are prevented. The thermal conductivity of MoW alloys is reduced for temperatures up to 1000 °C.

The special surface treatment and conditioning of pressed-sintered materials is presented. This process leads to smoothening and densification of the surface. By high-temperature exposure a coarse-grained structure is formed at the worked surface which is ideal for crucibles to improve their corrosion resistance against alumina melt. Together with the densified surface layer the high-temperature creep resistance is improved, too. Moreover, this technology leads to reduced gas bubble formation in the melt which increases the sapphire yield. Our wetting angle measurements confirm that Mo is the appropriate material selected for die-packs used in the EFG crystal growth method. However further studies particularly of the chemical interactions of alumina melt on refractory metals at high-temperature are required. Full understanding might allow to find non-wetting refractory materials. Combining this knowledge with the reduced CTE of MoW alloys as observed might pave the way for realizing re-useable crucibles as requested for the HEM crystal growth technology.

Acknowledgment

In this work the studies of wetting angles were supported by the Institut für Festkörperphysik of the Technical University of Vienna. The authors would like to thank Prof. Dr. Christoph Eisenmenger-Sittner and Christoph Tscherne, who carried out the wetting angle measurements.

References

1. E. R. Dobrovinskaya, L. A. Lytvynov, and V. Pishchik, Sapphire Material, Manufacturing, Applications, Springer, New York, (2009)
2. H. J. Scheel, and P. Capper, Crystal Growth Technology, Wiley-VCH, Weinheim, (2008)
3. H. Czichos, T. Saito, L. Smith, Handbook of Materials Measurement Methods, pp. 399–429, Springer, Heidelberg, (2006)
4. Y. Waseda, K. Hirata, and M. Ohtani, High-temperature thermal expansion of platinum, tantalum, molybdenum, and tungsten measured by x-ray diffraction, High Temperatures - High Pressures 7(2), 221–226, (1975)

5. W. J. Parker, R. J. Jenkins, C. P. Butler, G. L. Abott, Flash Method of Determining Thermal Diffusivity, Heat Capacity, and Thermal Conductivity, J. Appl. Phys. 32(9), 1679–1684, (1961)
6. P. Schoderböck, H. Klocker, L. S. Sigl, and G. Seeber, Evaluation of the Thermal Diffusivity of Thin Specimens from Laser Flash Data, Int. J. Thermophys. 30(2), 599–607, (2009)
7. T. M. Tritt, Thermal Conductivity Theory, Properties and Applications, Kluwer Academic/Plenum Publishers, New York, (2004)
8. T. Tanabe, C. Eamchotchawalit, C. Busabok, S. Taweethavorn, M. Fujitsuka, and T. Shikama, Temperature dependence of thermal conductivity in W and W–Re alloys from 300 to 1000 K, Mat. Let. 57, 2950–2953, (2003)
9. C. Miyagawa T. Kobayashi, T. Taishi, and K. Hoshikawa, Demonstration of crack-free c-axis sapphire crystal growth using the vertical Bridgman method, J. Crys. Gro. 372, 95–99, (2013)
10. M. Mark, H. Traxler, R. Schiftner, and W. Knabl, Glasschmelz-Komponente, Gebrauchsmuster AT GM 15.262, (2017)
11. C. Tscherne and C. Eisenmenger-Sittner, Hochtemperaturbenetzung von Aluminiumoxid auf Refraktärmetallen, Diplomarbeit am Institut für Festkörperphysik, Technische Universität Wien, (2016)